

### Acknowledgment

This work was performed under the sponsorship of the U.S. Air Force under Contract F49620-79-C-0054.

### References

- <sup>1</sup>Nixon, D., "Perturbation of a Discontinuous Transonic Flow," *AIAA Journal*, Vol. 16, Jan. 1978, pp. 47-52.
- <sup>2</sup>Nixon, D., "Perturbations in Two and Three Dimensional Transonic Flows," *AIAA Journal*, Vol. 16, July 1978, pp. 699-709.
- <sup>3</sup>Nixon, D. and Kerlick, G. D., "Perturbations of a Transonic Flow with Vanishing Shock Waves," Nielsen Engineering & Research, Inc., Mountain View, Calif., Paper 153, 1982.
- <sup>4</sup>Nixon, D., "Calculations of Transonic Flow Using the Integral Equation Method," Ph.D. Thesis, University of London, England, 1976.
- <sup>5</sup>Ballhaus, W. F. and Goorjian, P. M., "Implicit Finite-Difference Computations of Unsteady Transonic Flows About Airfoils Including the Effect of Irregular Shock Motions," *AIAA Journal*, Vol. 15, 1977, pp. 1728-1735.

## Upstream Influence in Conically Symmetric Flow

D. S. Dolling\*

The University of Texas at Austin, Austin, Texas

### Introduction

IN sharp fin-induced flows, where a swept planar shock wave interacts with a turbulent boundary layer, experimental results<sup>1-3</sup> show that outside of an inception zone near the fin leading edge, the interaction footprint is conically symmetric. Conically symmetric means that surface features, such as the line of upstream influence, lie along rays which intersect the trace of the inviscid shock wave at a common origin. This, and the coordinate system used in this Note, are shown in Fig. 1. The origin, as shown, may be a virtual one offset by distance  $\Delta L_s$  from the leading edge or the leading edge itself. In the conically symmetric regime, the spanwise growth of upstream influence,  $L_{u_n}$ , can be expressed in normalized form as

$$L_{u_n}/(L_s + \Delta L_s) = \tan(\beta_u - \beta_s) \quad (1)$$

where  $\beta_u$  and  $\beta_s$  are the angles of the line of upstream influence and the shock wave, respectively (Fig. 1).

Although this is a very simple formulation, it cannot be used in a predictive way unless  $\beta_u$  is known ( $\beta_s$  is calculated from the freestream Mach number  $M_\infty$  and the fin angle of attack  $\alpha$ ). The focus of the present work is to examine the available experimental data and determine the relationship between  $\beta_u$  and  $\beta_s$ . The data used are from the four studies given in Table 1.

The Mach 2 and 3 tests were made under adiabatic wall temperature conditions. Those at Mach 6 were made with a cooled wall (the wall to recovery temperature ratio was 0.5). The data of McCabe<sup>6</sup> ( $M_\infty = 2.95$ ), Peake<sup>7</sup> ( $M_\infty = 2$ ), Kubota<sup>8</sup> ( $M_\infty = 2.36, 2.41$ ), and Lowrie<sup>9</sup> ( $M_\infty = 3.44$ ) were also examined, but were judged to be within the inception zone, and thus have not been used.

### Discussion of Results

Upstream influence was determined from wall-pressure data at  $M_\infty = 2$  and 6 and from pressure data and surface streak patterns at  $M_\infty = 3$ . In all cases, inviscid shock theory was used to calculate  $\beta_s$ . Figure 2 shows  $\beta_u$  vs  $\beta_s$ . It is estimated that the accuracy of  $\beta_u$  is  $\pm 1$  deg. The larger errors are for small  $\alpha$  and are due more to uncertainty in locating the upstream influence line than in measuring a smaller angle. The flagged data at Mach 3 were obtained recently<sup>10</sup> in tests carried out under the same freestream conditions as Ref. 5. The hatched lines are discussed shortly.

At Mach 6, straight lines can be fitted through the upstream influence points and the fin leading edge at all  $\alpha$ , indicating that the entire flowfield is conically symmetric. This can also be seen in the sketches of the surface streak patterns, shown in Ref. 1. With  $\Delta L_s = 0$  Eq. (1) becomes

$$L_{u_n}/L_s = \tan(\beta_u - \beta_s) \quad (2)$$

With results from only one set of tests, it is not clear if this is a general result in hypersonic flow, the result of cold-wall conditions, or simply specific to this experiment. A second observation is that  $\beta_u$  increases with  $Re_{\delta_0}$ . Since the trend is weak, it is difficult to judge whether this is a real effect or a small systematic experimental error. It does not appear to be the result of viscous effects at the fin leading edge, since the opposite trend with Reynolds number would be expected.

In Fig. 2, the intersection point of each data set with the shock line is different since the Mach angle  $\mu$  depends on  $M_\infty$ . Further, in this coordinate system, a characteristic feature of the swept shock flowfield is effectively masked. To bring this feature out, obtain a common origin, and see more directly the influence of  $M_\infty$  on the relation between  $\beta_u$  and  $\beta_s$ , the data have been replotted as  $\Delta\beta = (\beta_u - \beta_s)$  vs  $\beta_s - \mu$  (Fig. 3).

For stronger shocks,  $(\beta_s - \mu) > \approx 6-8$  deg, it can be seen that the relationship between  $\Delta\beta$  and  $(\beta_s - \mu)$  is essentially linear at both Mach 3 and 6. In neither case does the best-fit straight line pass through the origin (this is most apparent at Mach 6). Although the increased data scatter makes it more difficult to

Table 1 Conically symmetric studies analyzed

Mach No.	$\delta_0$ , cm	$Re_{\delta_0} \times 10^6$	$C_f$	$\alpha$ , deg	Refs.
2	0.36	0.24	0.00169	4-8	4
3	0.44	0.29	0.00144	2-20	5, 10
6	0.37	0.12	—	6-16	1
6	0.30	0.30	—	6-16	1

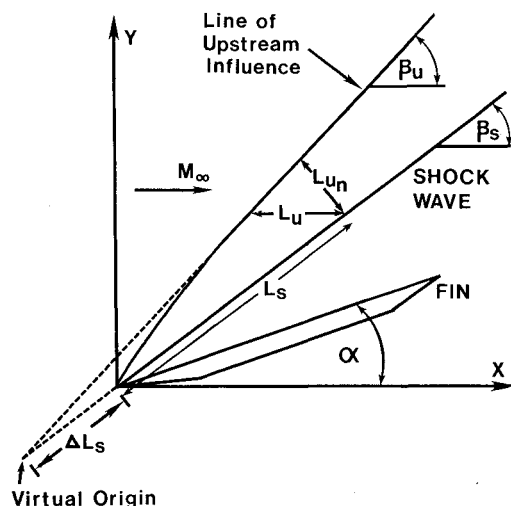


Fig. 1 Model and coordinate system.

Received March 28, 1984; revision received May 18, 1984. Copyright © American Institute of Aeronautics and Astronautics, Inc., 1985. All rights reserved.

\*Assistant Professor, Department of Aerospace Engineering and Engineering Mechanics.

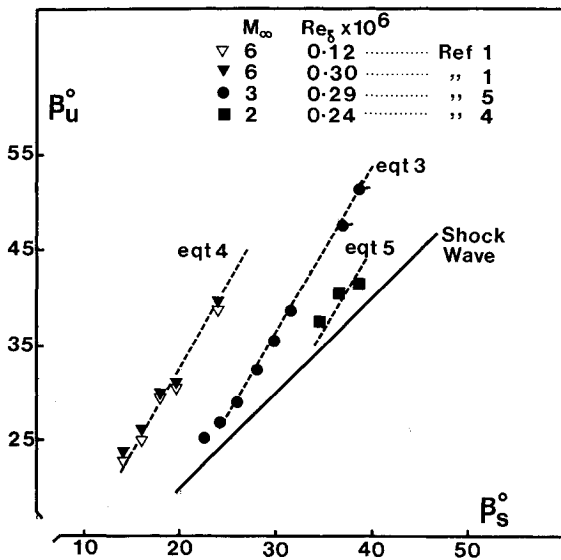


Fig. 2  $\beta_u$  vs  $\beta_s$  in conically symmetric region.

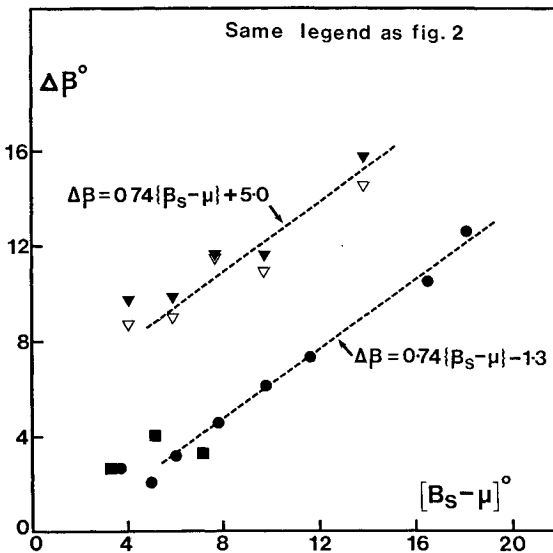


Fig. 3  $\Delta\beta$  vs  $(\beta_s - \mu)$  in conically symmetric region.

discern trends for the weaker shocks, single-point measurements of upstream influence at low  $\alpha$  (from which only very approximate estimates of  $\beta_u$  could be obtained), suggest that  $\Delta\beta$  remains relatively large and does not decrease rapidly until  $(\beta_s - \mu)$  is close to zero. At Mach 3, for example, upstream influence at  $\beta = 1$  deg (shock pressure ratio  $P_2/P_1 = 1.08$ ) is, at a given  $L_s$ , still 70% of the value at  $\alpha = 14$  deg ( $P_2/P_1 = 2.62$ ).

The physical reason for this stems from the inviscid-dominated character of these flows. Flowfield surveys<sup>11</sup> at Mach 3 have shown an extensive external compression wave system whose length scale is only weakly dependent on shock wave strength. Numerical simulations,<sup>12,13</sup> which are in good quantitative agreement with the experiment, support this. For relatively weak shocks, neither the experiments nor the computations show the presence of viscous dominated phenomena such as the characteristic reversed flow regions of two-dimensional separated flows.

The equations for the straight-line portions of the curve are given in Fig. 2. Use of the appropriate values of  $\mu$  gives

$$\beta_u = 1.74\beta_s - 10 \text{ deg} \quad (M_\infty = 3) \quad (3)$$

$$\beta_u = 1.74\beta_s - 2.2 \text{ deg} \quad (M_\infty = 6) \quad (4)$$

Equations (3) and (4) are shown by the hatched lines in Fig. 2. In this coordinate system, the departure from linearity at small  $\alpha$  is barely detectable. The Mach 2 data (Fig. 3) are not, strictly speaking, in the linear regime of the  $\Delta\beta$  vs  $\beta_s - \mu$  relationship, but the fact that use of the Mach 3 relation (with the proper value of  $\mu$ ), i.e.,

$$\beta_u = 1.74\beta_s - 24 \text{ deg} \quad (5)$$

passes through the data points suggests that the slope at Mach 2 will be about the same as at Mach 3 and 6. Additional experimental data are still needed to clarify this.

### Concluding Remarks

An examination has been made of experimental upstream influence data in the conically symmetric regime of sharp fin-induced shock-wave/turbulent boundary-layer interaction. For the cases examined, which were adiabatic wall supersonic flows and cold-wall, moderately hypersonic flows, the results show that the growth of upstream influence  $L_{uq}$  with distance  $L_s$  along the shock wave can be expressed as a linear function of the shock wave angle  $\beta_s$ . That the upstream influence can be expressed in terms of a single inviscid parameter further supports the idea that such interactions are governed primarily by inviscid mechanisms. An area requiring further study is that of the inception zone. In the hypersonic test case the virtual origin and leading edge were found to be coincident, whereas in supersonic flow<sup>2-11</sup> there is always a curved inception zone. Since the absence of this zone simplifies the relationship between  $L_{uq}$  and  $\beta_s$ , then learning which parameters control its shape and scale would be a useful practical result.

### Acknowledgment

The Mach 2 and 3 experiments were carried out while the author was a Research Staff member at the Gas Dynamics Laboratory at Princeton University, and were part of a study supported by A.F.O.S.R. under Contract F49620-81-0018, monitored by Dr. James Wilson.

### References

- Law, H. C., "Three Dimensional Shock Wave Turbulent Boundary Layer Interactions at Mach 6," U.S. Air Force Aerodynamics Research Laboratory, TR-75-0191, June 1975.
- Settles, G. S., Perkins, J. J., and Bogdonoff, S. M., "Upstream Influence Scaling of 2D and 3D Shock/Turbulent Boundary-Layer Interactions at Compression Corners," *AIAA Journal*, Vol. 20, June 1982, pp. 782-789.
- Lu, F. and Settles, G. S., "Conical Similarity of Shock Boundary-Layer Interactions Generated by Swept Fins," *AIAA Paper* 83-1756, July 1983.
- Dolling, D. S., "Effects of Mach Number on Upstream Influence in Sharp Fin-Induced Shock Wave Turbulent Boundary Layer Interaction," *AIAA Paper* 84-0095, Jan. 1984.
- Dolling, D. S. and Bogdonoff, S. M., "Upstream Influence in Sharp Fin-Induced Shock Wave Turbulent Boundary Layer Interaction," *AIAA Journal*, Vol. 21, 1983, pp. 143-145.
- McCabe, A., "Study of Three Dimensional Interactions Between Shock Waves and Turbulent Boundary Layers," Ph.D. Thesis, University of Manchester, U.K., 1963.
- Peake, D. J., "The Three Dimensional Interaction of a Swept Shock Wave with a Turbulent Boundary Layer and the Effects of Air Injection on Separation," Ph.D. Thesis, Carleton University, Ottawa, Canada, 1975.
- Kubota, H., "Investigations of Three-Dimensional Shock Wave Boundary Layer Interactions," Cranfield College of Aeronautics, Rept. 8001, Jan. 1980.
- Lowrie, B. W., "Cross Flows Produced by the Interaction of Swept Shock Wave with a Turbulent Boundary Layer," Ph.D. Thesis, Cambridge University, U.K., 1965.
- Goodwin, S. and Bogdonoff, S. M., private communication, Gas Dynamics Laboratory, Princeton University, Princeton, N.J., 1984.

<sup>11</sup>Oskam, B., Bogdonoff, S. M., and Vas, I. E., "Study of Three Dimensional Flow Fields Generated by the Interactions of a Skewed Shock Wave with the Turbulent Boundary Layer," AFFDL-TR-75-21, Feb. 1975.

<sup>12</sup>Horstman, C. C. and Hung, C. M., "Computation of Three Dimensional Turbulent Separated Flows at Supersonic Speeds," AIAA Paper 79-0002, Jan. 1979.

<sup>13</sup>Knight, D. D., "A Hybrid Explicit-Implicit Numerical Algorithm for the Three-Dimensional Compressible Navier-Stokes Equations," AIAA Paper 83-0223, Jan. 1983.

## Improved Series Solutions of Falkner-Skan Equation

Noor Afzal\*

Aligarh Muslim University, Aligarh, India

### Introduction

RECENTLY, Aziz and Na<sup>1</sup> studied a series solution of the Falkner-Skan equation

$$f''' + ff'' + \beta(1 - f'^2) = 0 \quad (1)$$

$$f(0) = f'(0) = 0, \quad f'(\infty) = 1 \quad (2)$$

by expanding the nondimensional stream function  $f$  in the powers of  $\beta$  as

$$f = \sum_{n=0}^{\infty} \beta^n f_n(\eta) \quad (3)$$

The lowest order term in Eq. (3) satisfies the Blasius equation

$$f_0''' + f_0 f_0'' = 0 \quad (4)$$

$$f_0(0) = f_0'(0) = 0, \quad f_0'(\infty) = 1 \quad (5)$$

and the higher order perturbations by the recurrence relation

$$f_n''' + f_0 f_n'' + f_0' f_n' = -\delta_{in} + \sum_{r=1}^n f_{r-1}' f_{n-r}' - \sum_{r=1}^{n-1} f_r f_{n-r}'' \quad (6)$$

$$f_n(0) = f_n'(0) = 0, \quad f_n'(\infty) = 0 \quad (7)$$

where  $\delta_{ij}$  is the well-known Kronecker delta. The first 11 terms in the expansion have been estimated and the result for skin friction is

$$f''(0) = \sum_{n=0}^{\infty} A_n \beta^n \quad (8)$$

where the values of  $A_n$  are given in Table 1. For certain specific values of  $\beta$  in the range  $-\beta_s < \beta \leq 2$ , where

$$\beta_s = 0.198838$$

the results of Eq. (8) were improved by Shanks' transformation. The predictions are in good agreement with exact numerical solutions. However, the range of interest for values of  $\beta$  covers  $-\beta_s$  to infinity (see Afzal and Luthra<sup>2</sup> and

Evans<sup>3</sup>). Therefore, it is advantageous to improve the convergence of Eq. (8) for a general value of  $\beta$  rather than for the specific values considered by Aziz and Na.<sup>1</sup>

### Analysis of the Series

The aim of this Note is to improve the convergence of Eq. (8) by Euler transformation and completing it by determining the remainder. An insight into the location of the nearest singularity can be gained by studying the radius of its convergence (say,  $\beta_0$ ), defined by D'Alembert's ratio test

$$\beta_0 = \lim_{n \rightarrow \infty} |A_{n-1}/A_n| \quad (9)$$

Domb and Sykes<sup>4</sup> have observed that D'Alembert's limit hopefully can be estimated from a finite number of coefficients by plotting the inverse ratios  $A_n/A_{n-1}$  against  $1/n$  (known as the Domb-Sykes plot) and extrapolating to  $1/n = 0$ . The Domb-Sykes plot has the advantage that, for certain common types of functions, the extrapolation turns out to be linear. For example, for the following functions,

$$F = \text{const} \begin{cases} (\beta_0 \pm \beta)^a, & a \neq 0, 1, \dots \\ (\beta_0 \pm \beta)^a \log(\beta_0 \pm \beta), & a = 0, 1, \dots \end{cases} \quad (10a)$$

$$(10b)$$

the inverse coefficients, in the expansion  $F = \sum A_n \beta^n$ ,

$$\frac{A_n}{A_{n-1}} = \mp \frac{1}{\beta_0} \left( 1 - \frac{1+a}{n} \right) \quad (11)$$

is exactly linear in  $1/n$ . For more complicated functions the nearest singularity has a leading term similar to Eq. (10) and the ratio  $A_n/A_{n-1}$  will behave asymptotically linearly, such as Eq. (11) for large  $n$ . The slope of the Domb-Sykes plot gives the nature of the singularity and the inverse of the intercept gives its location.

The Domb-Sykes plot for Eq. (8), shown in Fig. 1, is almost linear. An extrapolation to  $1/n$ , shown by the line in the figure, leads to the value  $1/\beta_0 = 5.03$  or  $\beta_0 = 0.1988$ , which within the graphical accuracy shows  $\beta_0 = \beta_s$ . The slope of the line leads to  $a = 1/2$ . Therefore, from the Domb-Sykes plot in Fig. 1, we get

$$\beta_0 = \beta_s = 0.198838, \quad a = 1/2 \quad (12)$$

Equation (12) shows that Eq. (8) possesses the square root singularity on the real axis in the complex  $\beta$  plane at  $\beta = \pm \beta_0$ .

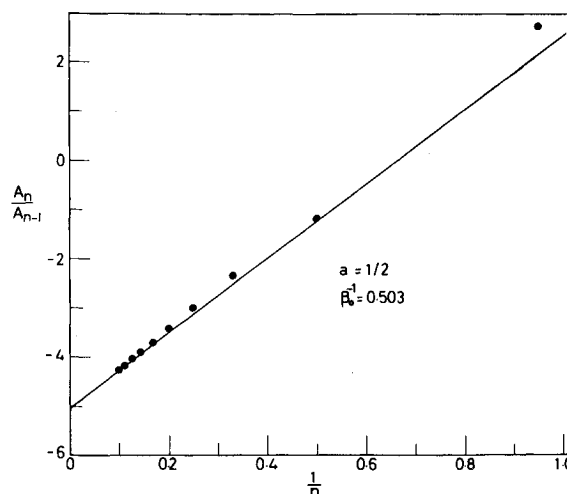


Fig. 1 Domb-Sykes plot for Eq. (8).